Available online at www.sciencedirect.com

SCIENCE DIRECT®

International Journal of Heat and Mass Transfer 48 (2005) 4963–4972

International Journal of HEAT and MASS TRANSFER

www.elsevier.com/locate/ijhmt

The effects of variable properties and hall current on steady MHD laminar convective fluid flow due to a porous rotating disk

Kh. Abdul Maleque [a,*], Md. Abdus Sattar [b]

[a] *Department of Mathematics, American International University-Bangladesh, House-53/B, 21, Kemal Ataturk Avenue, Banani, Dhaka-1213, Bangladesh*

[b] *Department of CSE, North South University, 12 Kemal Ataturk Avenue, Banani, Dhaka-1213, Bangladesh*

Received 15 June 2004; received in revised form 11 November 2004
Available online 28 July 2005

Abstract

The present investigation is concerned with the effects of variable properties [density (ρ), viscosity (μ) and thermal conductivity (κ)], Hall current (m), magnetic field (M) and suction/injection (W_s) on steady MHD laminar flow of an electrically conducting fluid on a porous rotating disk in presence of a uniform magnetic field. The fluid properties are taken to be strong functions of temperature. The induced magnetic field is neglected while the electron–atom collision frequency is assumed to be relatively high, so that the Hall effect is assumed to exist. The dimensionless steady governing equations are then solved numerically by using Runge–Kutta and Shooting method, and the effects of the relative parameters are examined.

1. Introduction

Rotating disk flow along with heat transfer is one of the classical problems of fluid mechanics, which has both theoretical and practical value. The importance of heat transfer from a rotating body can be ascertained in cases of various types of machinery, for example computer disk derives (see [1]) and gas turbine rotors (see [2]).

The rotating-disk problem was first formulated by von-Karmann [3]. He has shown that Navier–Stokes equations of steady flow of a viscous incompressible fluid due to an infinite rotating disk can be reduced to a set of ordinary differential equations and solved them by approximate integral method. But Cochran [4] pointed out that von-Karman's momentum integral solution contained errors. He obtained more accurate results by patching two series expansions. It has been found that the disk acts like a centrifugal fan and hence the fluid near the surface being thrown radially upwards. This in turn generates an axial flow towards the disk to maintain continuity. Benton [5], further improved Cochran's solution and extended the hydrodynamic problem to the flow starting impulsively from rest. The rotationally symmetric flow in presence of an infinite rotating disk with different angular velocity was studied by Roger and Lance [6]. Following a suggestion made by Batchelor [7], Stuart [8] investigated the effect of uniform suction of fluid from

* Corresponding author.
E-mail addresses: khmaleque@yahoo.com (Kh. Abdul Maleque), asattar@northsouth.edu (Md. Abdus Sattar).

0017-9310/$ - see front matter © 2005 Elsevier Ltd. All rights reserved.
doi:10.1016/j.ijheatmasstransfer.2005.05.017

the surface of a rotating disk. Suction essentially decreases both the radial and azimuthal components of velocity but increases the axial flow towards the disk at infinity. As a consequence, the boundary layer becomes thinner. Ockendon [9] used asymptotic method to determine the solutions of the problem for small values of suction parameter in case of a rotating disk in a rotating fluid. On the other hand, the effect of uniform blowing through a rotating porous disk on the flow induced by this disk was studied by Kuiken [10].

Some interesting results on the effects of the magnetic field on the steady flow due to the rotation of a disk of infinite or finite extent was pointed out by El-Mistikawy et al. [11,12]. Hassan and Attia [13] investigated the steady magneto-hydrodynamic boundary layer flow due to an infinite disk rotating with uniform angular velocity in the presence of an axial magnetic field. They neglected the induced magnetic field but considered Hall current and accordingly solved steady state equations numerically using finite difference approximation. Attia [14] investigated the effects of suction as well as injection along with effects of magnetic field in a flow near a rotating porous disk. It was observed by him that strong injection tends to destabilize the laminar boundary layer but when magnetic field works along with even strong injection, it stabilizes the boundary layer.

In all the above studies to the authors' knowledge, constant properties of fluid were not assumed. However, it is known that these physical properties may change significantly with temperature of the flow. To predict the flow behavior accurately, it may be necessary to take into account these variable properties. In this light Zakerullah and Ackroyd [15] investigated the free convection flow above a horizontal circular disk for variable fluid properties. Herwig [16] analyzed the influence of variable properties on laminar fully developed pipe flow with constant heat flux across the wall. It was shown how the exponents in the property ratio method depend on the fluid properties. The influence of temperature dependent fluid properties on laminar boundary layers was examined by Herwig and Wickern [17] for wedge flow. In case of fully developed laminar flow in concentric annuli, the effect of the variable property has been studied by Herwig and Klemp [18]. Herwig [19] studied the laminar film boiling including variable properties.

In the present paper, the steady MHD laminar flow of a viscous conducting, compressible flow due to a porous rotating disk of infinite extend is studied in the presence of an external uniform magnetic field directed perpendicular to the disk taking the properties of the fluid as strong functions of temperature. A uniform suction or injection through the disk is considered for the whole range of suction or injection velocities. The governing non-linear partial differential equations are integrated numerically using Nachtsheim and Swigert [20] iteration technique.

2. Basic equations

Consider the steady MHD laminar boundary layer flow due to a rotating disk in an electrically conducting viscous compressible fluid in the presence of an external magnetic field and Hall current. The equations governing the fluid flow are

Equation of continuity : $\nabla.(\rho \boldsymbol{q}) = 0,$ (1)

Navier–Stokes equation :

$$\rho(\boldsymbol{q}.\nabla)\boldsymbol{q} = -\nabla p + [\nabla.(\mu\nabla)]\boldsymbol{q} + (\boldsymbol{J}\times\boldsymbol{B}), \quad (2)$$

The generalized Ohm's law :

$$\boldsymbol{J} = \sigma[\boldsymbol{E} + \boldsymbol{q}\times\boldsymbol{B} - \beta(\boldsymbol{J}\times\boldsymbol{B})], \quad (3)$$

Energy equation : $\rho C_p(\boldsymbol{q}.\nabla)T = \nabla.(\kappa\nabla)T.$ (4)

The external uniform magnetic field is applied perpendicular to the plane of the disk and has a constant magnetic flux density $\boldsymbol{B} = (0, 0, B_0)$ which is assumed unaltered by taking magnetic Reynold's number $Re_{\rm m} \ll 1$. $\boldsymbol{E}$ is the electric field which results from charge separation and is in the z-direction. Eq. (3) expresses the Hall effect, where $\beta = \frac{1}{ne}$ is the Hall factor, n is the electron concentration per unit volume and $-e$ is the charge of electron. In Eq. (4), we neglected the viscous energy dissipation, Joule heating term and the heat generation/absorption coefficient.

3. Governing equations

Using non-rotating cylindrical polar coordinates (r, ϕ, z), the disk rotates with constant angular velocity Ω and is placed at $z = 0$, and the fluid occupies the region $z > 0$, where z is the vertical axis in the cylindrical coordinates system with r and ϕ as the radial and tangential axes respectively. The components of the flow velocity $\boldsymbol{q}$ are (u, v, w) in the directions of increasing (r, ϕ, z) respectively, the pressure is P and the density of the fluid is ρ. T is the fluid temperature and the surface of the rotating disk is maintained at a uniform temperature $T_{\rm w}$. Far away from the wall, the free stream is kept at a constant temperature T_∞ and at a constant pressure P_∞. The fluid is assumed to be Newtonian, viscous and electrically conducting. The external uniform magnetic field is applied perpendicular to the surface of the disk and has a constant magnetic flux density B_0 which is assumed unchanged by taking small magnetic Reynolds number ($Re_{\rm m} \ll 1$). The electron–atom collision frequency is assumed to be relatively high, so that the Hall effect is assumed to exist. We assume that the fluid properties, viscosity (μ) and thermal conductivity (κ) coefficients and density (ρ) are functions of temperature alone and obey the following laws [21]:

$$\mu = \mu_\infty[T/T_\infty]^a, \quad \kappa = \kappa_\infty[T/T_\infty]^b \quad \text{and}$$
$$\rho = \rho_\infty[T/T_\infty]^d, \quad (5)$$

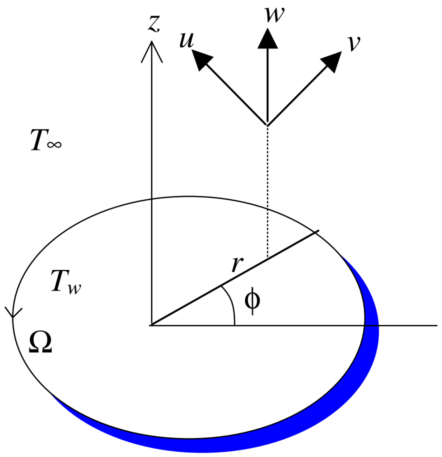

Fig. 1. The flow configuration and the coordinate system.

where the a, b and d are arbitrary exponents, κ_∞ is an uniform thermal conductivity of heat and μ_∞ is a uniform viscosity of a fluid. For the present analysis fluid considered is flue gas. For flue gases the values of the exponents a, b and d are taken as $a = 0.7$, $b = 0.83$ and $d = -1.0$.

The physical model and geometrical coordinates are shown in Fig. 1. Due to steady axially symmetric, compressible MHD laminar flow of a homogeneous fluid the governing equations take the following form from Eq. (1)–(4) as:

$$\frac{\partial}{\partial r}(\rho r u) + \frac{\partial}{\partial z}(\rho r w) = 0, \tag{6}$$

$$\rho\left(u\frac{\partial u}{\partial r} - \frac{v^2}{r} + w\frac{\partial u}{\partial z}\right) + \frac{\sigma B_0^2}{(1+m^2)}(u - mv) + \frac{\partial P}{\partial r} = \frac{\partial}{\partial r}\left(\mu\frac{\partial u}{\partial r}\right) + \frac{\partial}{\partial r}\left(\mu\frac{u}{r}\right) + \frac{\partial}{\partial z}\left(\mu\frac{\partial u}{\partial z}\right), \tag{7}$$

$$\rho\left(u\frac{\partial v}{\partial r} + \frac{uv}{r} + w\frac{\partial v}{\partial z}\right) + \frac{\sigma B_0^2}{(1+m^2)}(v + mu) = \frac{\partial}{\partial r}\left(\mu\frac{\partial v}{\partial r}\right) + \frac{\partial}{\partial r}\left(\mu\frac{v}{r}\right) + \frac{\partial}{\partial z}\left(\mu\frac{\partial v}{\partial z}\right), \tag{8}$$

$$\rho\left(u\frac{\partial w}{\partial r} + w\frac{\partial w}{\partial z}\right) + \frac{\partial P}{\partial z} = \frac{\partial}{\partial r}\left(\mu\frac{\partial w}{\partial r}\right) + \frac{1}{r}\frac{\partial}{\partial r}(\mu w) + \frac{\partial}{\partial z}\left(\mu\frac{\partial w}{\partial z}\right), \tag{9}$$

$$\rho C_p\left(u\frac{\partial T}{\partial r} + w\frac{\partial T}{\partial z}\right) = \frac{\partial}{\partial r}\left(\kappa\frac{\partial T}{\partial r}\right) + \frac{\kappa}{r}\frac{\partial T}{\partial r} + \frac{\partial}{\partial z}\left(\kappa\frac{\partial T}{\partial z}\right), \tag{10}$$

here, σ is the electrical conductivity, C_p is the specific heat at constant pressure and m is the Hall current.

Appropriate boundary conditions for the flow induced by an infinite disk ($z = 0$) which is started impulsively into steady rotation with constant angular velocity Ω and a uniform suction/injection w_w through the disk, are given by

$$\left.\begin{array}{lllll} u = 0, & v = \Omega r, & w = w_w, & T = T_w & \text{at } z = 0 \\ u \to 0, & v \to 0, & T \to T_\infty & P \to P_\infty & \text{as } z \to \infty. \end{array}\right\} \tag{11}$$

4. Similarity transformations

To obtain the solutions of the governing equations, following von-Karmann, a dimensionless normal distance from the disk, $\eta = z(\Omega/\nu_\infty)^{\frac{1}{2}}$ is introduced along with the following representations for the radial, tangential and axial velocities, pressure and temperature distributions:

$$\left.\begin{array}{l} u = \Omega r F(\eta), \quad v = \Omega r G(\eta), \quad w = (\Omega\nu_\infty)^{\frac{1}{2}}H(\eta) \\ P - P_\infty = 2\mu_\infty\Omega p(\eta) \quad \text{and} \quad T - T_\infty = \Delta T\theta(\eta), \end{array}\right\} \tag{12}$$

where ν_∞ is a uniform kinematic viscosity of the fluid and $\Delta T = T_w - T_\infty$. Eqs. (6)–(8) and (10) in this case reduce to the system

$$H' + 2F + H\theta'(1+\gamma\theta)^{-1}\gamma d = 0, \tag{13}$$

$$F'' + a\gamma(1+\gamma\theta)^{-1}\theta' F' - \left[F^2 - G^2 + HF'\right](1+\gamma\theta)^{d-a} - \frac{M}{1+m^2}(F - mG)(1+\gamma\theta)^{-a} = 0, \tag{14}$$

$$G'' + a\gamma(1+\gamma\theta)^{-1}\theta' G' - (1+\gamma\theta)^{d-a}[2FG + HG'] - \frac{M}{1+m^2}(G + mF)(1+\gamma\theta)^{-a} = 0, \tag{15}$$

$$\theta'' + b\gamma(1+\gamma\theta)^{-1}\theta'^2 - Pr H\theta'(1+\gamma\theta)^{d-b} = 0, \tag{16}$$

where, $M = \sigma B_0^2/\Omega\rho_\infty$ is the magnetic parameter, $Pr = \mu_\infty C_p/\kappa_\infty$ is the Prandtl number and $\gamma = \Delta T/T_\infty$ is the relative temperature difference parameter, which is positive for a heated surface, negative for a cooled surface and zero for uniform properties. The boundary conditions (11) transform to

$$\left.\begin{array}{l} F(0) = 0, \quad G(0) = 1, \quad H(0) = W_s, \quad \theta(0) = 1, \\ F(\infty) = G(\infty) = \theta(\infty) = p(\infty) = 0 \end{array}\right\}, \tag{17}$$

where $W_s = w_w/\sqrt{\nu_\infty\Omega}$ and is obtained from Eq. (12). Here W_s represents a uniform suction ($W_s < 0$) or injection ($W_s > 0$) at the surface (see [22]).

5. Solutions

Numerical solutions to the transformed set of coupled, nonlinear, differential Eqs. (13)–(16) were obtained, utilizing a modification of the program suggested by Nachtsheim and Swigert. Within the context of the initial value method and the Nachtsheim–Swigert iteration technique the outer boundary conditions may be functionally represented by the first order Taylor's series as

$$\begin{aligned} F(\eta_{\max}) &= F(X,Y,Z) \\ &= F_0(\eta_{\max}) + \Delta X\,F_X + \Delta Y\,F_Y + \Delta Z\,F_Z = \delta_1, \\ G(\eta_{\max}) &= G(X,Y,Z) \\ &= G_0(\eta_{\max}) + \Delta X\,G_X + \Delta Y\,G_Y + \Delta Z\,G_Z = \delta_2, \\ \theta(\eta_{\max}) &= \theta(X,Y,Z) \\ &= \theta_0(\eta_{\max}) + \Delta X\,\theta_X + \Delta Y\,\theta_Y + \Delta Z\,\theta_Z = \delta_3, \end{aligned}$$

with the asymptotic convergence criteria given by

$$\begin{aligned} F'(\eta_{\max}) &= F'(X,Y,Z) \\ &= F'_0(\eta_{\max}) + \Delta X\,F'_X + \Delta Y\,F'_Y + \Delta Z\,F'_Z = \delta_4, \\ G'(\eta_{\max}) &= G'(X,Y,Z) \\ &= G'_0(\eta_{\max}) + \Delta X\,G'_X + \Delta Y\,G'_Y + \Delta Z\,G'_Z = \delta_5, \\ \theta'(\eta_{\max}) &= \theta'(X,Y,Z) \\ &= \theta'_0(\eta_{\max}) + \Delta X\,\theta'_X + \Delta Y\,\theta'_Y + \Delta Z\,\theta'_Z = \delta_6, \end{aligned}$$

where, $X = F'(0)$, $Y = G'(0)$, $Z = \theta'(0)$ and X, Y, Z subscripts indicate partial differentiation, e.g., $F_X = \frac{\partial F}{\partial F'(0)}$. The subscript *0* indicates the value of the function at $\eta_{\max}$ to be determined from the trial integration.

Solution of these equations in a least square sense requires determining the minimum value of $E = \delta_1^2 + \delta_2^2 + \delta_3^2 + \delta_4^2 + \delta_5^2 + \delta_6^2$ with respect to X, Y and Z. To solve ΔX, ΔY and ΔZ we require to differentiate E with respect to X, Y and Z respectively. Thus adopting this numerical technique, a computer program was set up for the solutions of the basic non-linear differential equations of our problem where the integration technique was adopted as a six ordered Range–Kutta method of integration. Various groups of the parameters γ, W_s, M and m were considered in different phases. In all the computations the step size $\Delta\eta = 0.01$ was selected that satisfied a convergence criterion of 10^{-6} in almost all of different phases mentioned above. Stating $\eta_\infty = \eta_\infty + \Delta\eta$, the value of η_∞ was found to each iteration loop. $(\eta_\infty)_{\max}$, to each group of the parameters, has been obtained when value of unknown boundary conditions at $\eta = 0$ not change to successful loop with error less than 10^{-6}. However, different step sizes such as $\Delta\eta = 0.01$, $\Delta\eta = 0.005$ and $\Delta\eta = 0.001$ were also tried and the obtained solutions have been found to be independent of the step sizes as observed in Fig. 2.

The skin friction coefficients and the rate of heat transfer to the surface, which are of chief physical interest, are also calculated out. The action of the variable properties in the fluid adjacent to the disk sets up a tangential shear stress, which opposes the rotation of the disk. As a consequence, it is necessary to provide a torque at the shaft to maintain a steady rotation. To find the tangential shear stress τ_t and surface (radial) stress τ_r, we apply the Newtonian formulae:

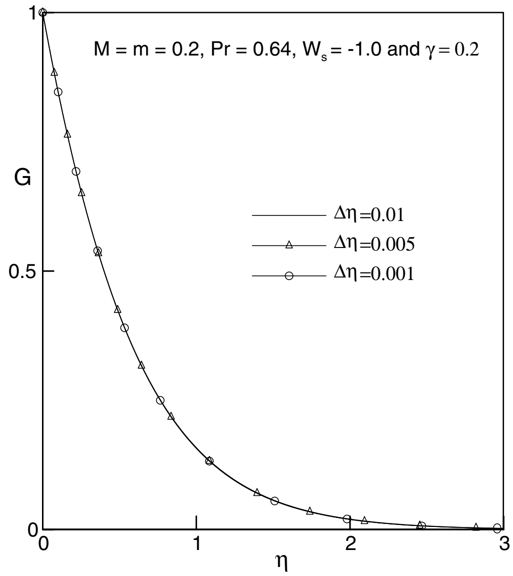

Fig. 2. Tangential velocity profiles for different step sizes.

$$\tau_t = \left[\mu\left(\frac{\partial v}{\partial z} + \frac{1}{r}\frac{\partial w}{\partial \phi}\right)\right]_{z=0} = \mu_\infty(1+\gamma)^a Re^{\frac{1}{2}}\Omega G'(0),$$

and

$$\tau_r = \left[\mu\left(\frac{\partial u}{\partial z} + \frac{\partial w}{\partial r}\right)\right]_{z=0} = \mu_\infty(1+\gamma)^a Re^{\frac{1}{2}}\Omega F'(0).$$

Hence the tangential and radial skin-frictions are respectively given by

$$(1+\gamma)^{-a} Re^{\frac{1}{2}} C_{f_t} = G'(0), \tag{18}$$

and

$$(1+\gamma)^{-a} Re^{\frac{1}{2}} C_{f_r} = F'(0). \tag{19}$$

The rate of heat transfer from the disk surface to the fluid is computed by the application of Fourier's law as given below

$$q = -\left(\kappa\frac{\partial T}{\partial z}\right)_{z=0} = -\kappa_\infty \Delta T(1+\gamma)^b \left(\frac{\Omega}{v_\infty}\right)^{\frac{1}{2}} \theta'(0).$$

Hence the Nusselt number (Nu) is obtained as

$$(1+\gamma)^{-b} Re^{-\frac{1}{2}} Nu = -\theta'(0), \tag{20}$$

where $Re(= \Omega r^2/v_\infty)$ is the rotational Reynolds number. In Eqs. (18)–(20), the gradient values of G, F and θ at the surface are evaluated when the corresponding differential equations are solved satisfying the convergence criteria.

6. Results and discussions

As a result of the numerical calculations, the velocity and temperature distributions for the flow are obtained from Eqs. (13)–(16) and are displayed in Figs. 3–6 for different values of γ (relative temperature difference parameter), W_s (suction /injection parameter), M (magnetic parameter) and m (Hall current) respectively. In the present analysis the fluid considered is flue gas. For flue gases ($Pr = 0.64$) the values of the exponents a, b and d are taken as $a = 0.7$, $b = 0.83$ and $d = -1.0$. $\gamma = \Delta T/T_\infty$ is termed as the relative temperature difference parameter, which is positive for a heated surface, negative for a cooled surface and zero for the case of constant property. In order to highlight the validity of the numerical computations adopted in the present investigation, some of our results for constant property case have been compared with those of Kelson and

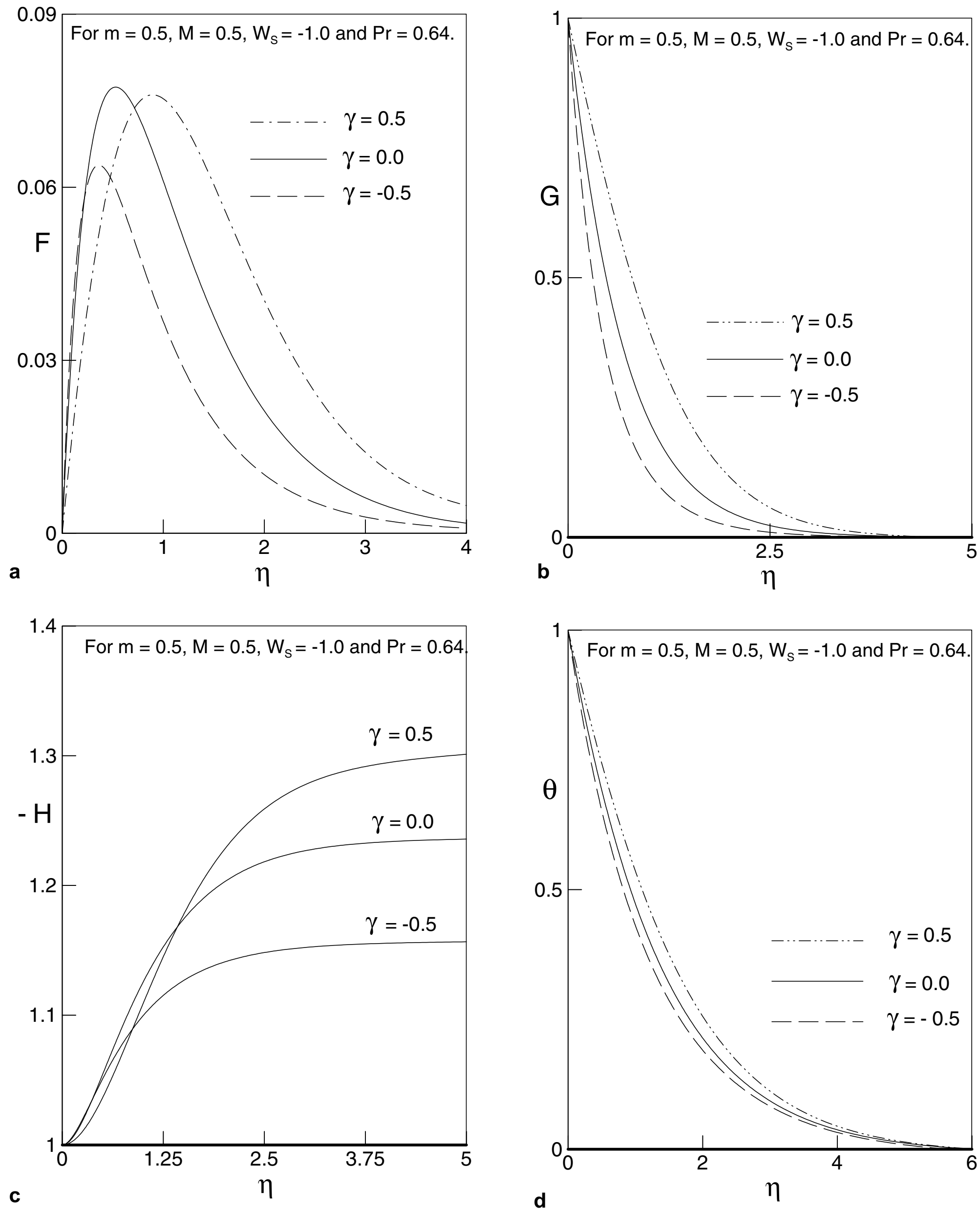

Fig. 3. (a) Effect of γ on the radial velocity profiles, (b) effect of γ on the tangential velocity profiles, (c) effect of γ on the axil velocity profiles and (d) effect of γ on the temperature velocity profiles.

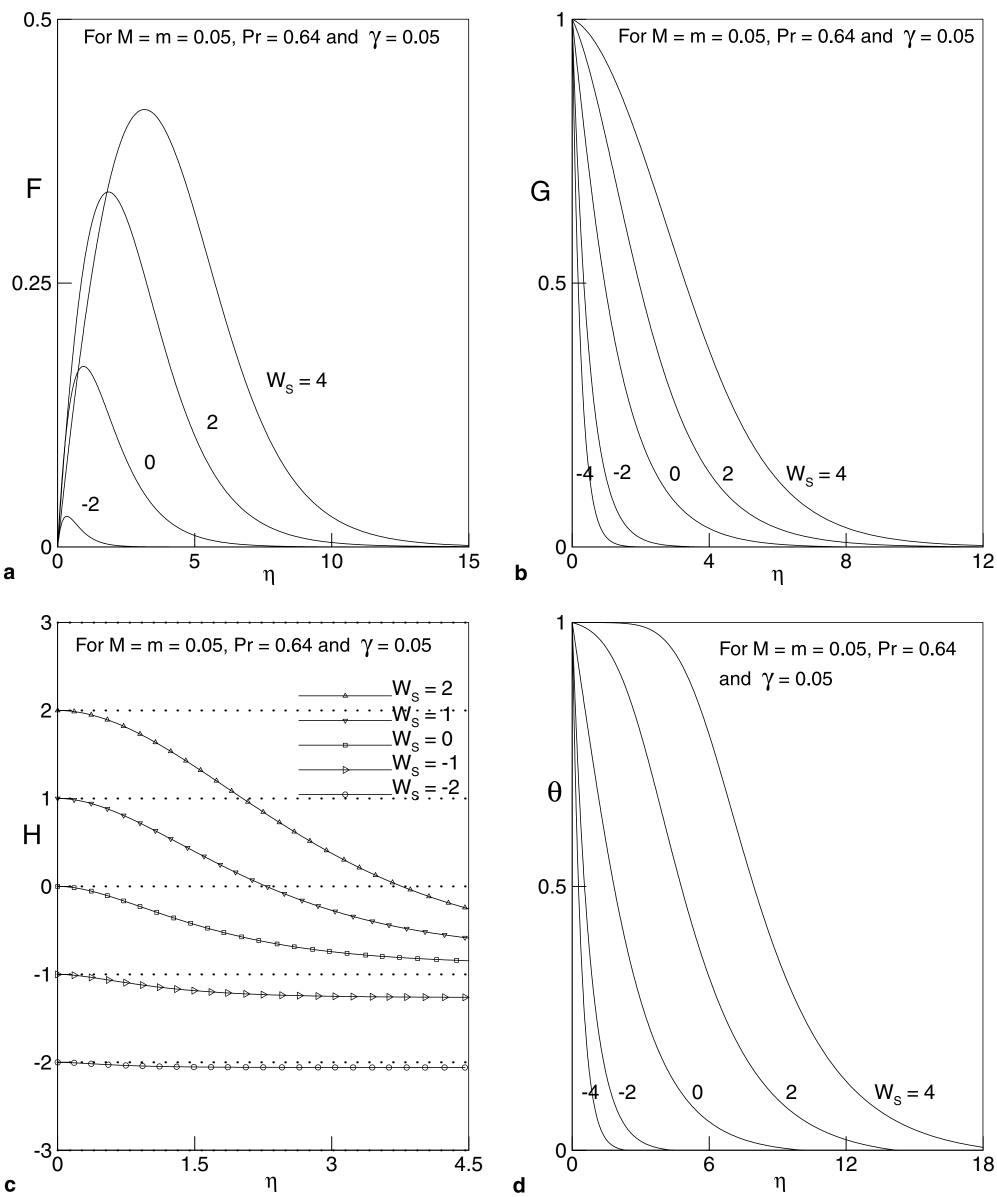

Fig. 4. (a) Effect of W_s on the radial velocity profiles, (b) effect of W_s on the tangential velocity profiles, (c) effect of W_s on the axial velocity profiles and (d) effect of W_s on the temperature velocity profiles.

Desseaux [22] in Table 1. The comparisons show excellent agreements, hence an encouragement for the use of the present numerical computations.

The effects of γ on the radial, tangential and axial velocity and temperature profiles are shown in Fig. 3(a)–(d). In these figures comparison is made between the constant property and variable property solutions. From Fig. 3(a), it is seen that due to existence of the centrifugal force the radial velocity attains a maximum value close to the surface of the disk for all values of γ. The largest maximum value of the velocity is attained in case of the constant property ($\gamma = 0$). Fig. 3(a) also shows that very close to the disk surface an increase in the values of γ leads to the decrease in the values of the radial velocity while for most part of the boundary layer at a fixed η position radial velocity increases with the increase of the relative temperature difference parameter γ. Similar effects of γ are also observed in case of axial velocity profiles (Fig. 3(c)). From Fig. 3(c) it is also observed that close to the disk surface the positive values of γ have a tendency to give rise to the familiar inflection point profiles, which indicates that

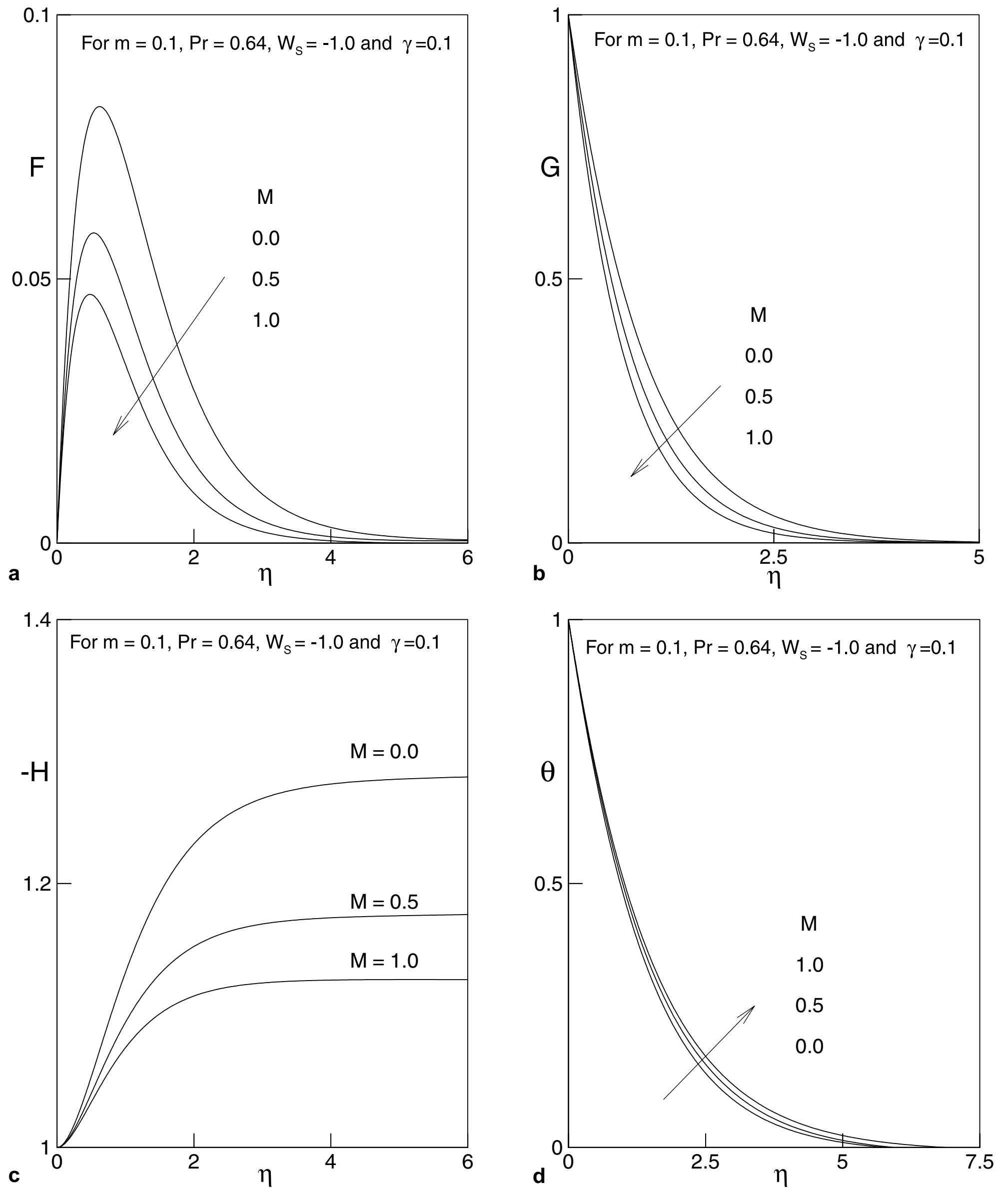

Fig. 5. (a) Effect of M on the radial velocity profiles, (b) effect of M on the tangential velocity profiles, (c) effect of M on the axial velocity profiles and (d) effect of M on the temperature velocity profiles.

variable property with highly heated surface may lead to the destabilization of the laminar flow resulting to the development of the viscous sub-layer. From Fig. 3(b), it is found that the tangential velocity increase with the increasing values of γ at a fixed point of the boundary layer. Fig. 3(d) shows that non-dimensional temperature increases with increasing values of γ, but the rate of increase is very small and hence the thermal boundary layer does not vary for solutions with the consideration of the property variations.

The effects of suction and injection (W_s) for $\gamma = 0.05$, $M = m = 0.05$ and $Pr = 0.64$ on the radial, the tangential, the axial velocity profiles and temperature profiles are shown in Fig. 4(a)–(d). For strong suction, the axial velocity is nearly constant; the radial velocity is very small while tangential velocity and temperature decay rapidly away from the surface. The fact that suction stabilizes the boundary layer is also apparent from these figures. As for the injection ($W_s > 0$), from Fig. 4(a)–(c) it is observed that the boundary layer is increasingly

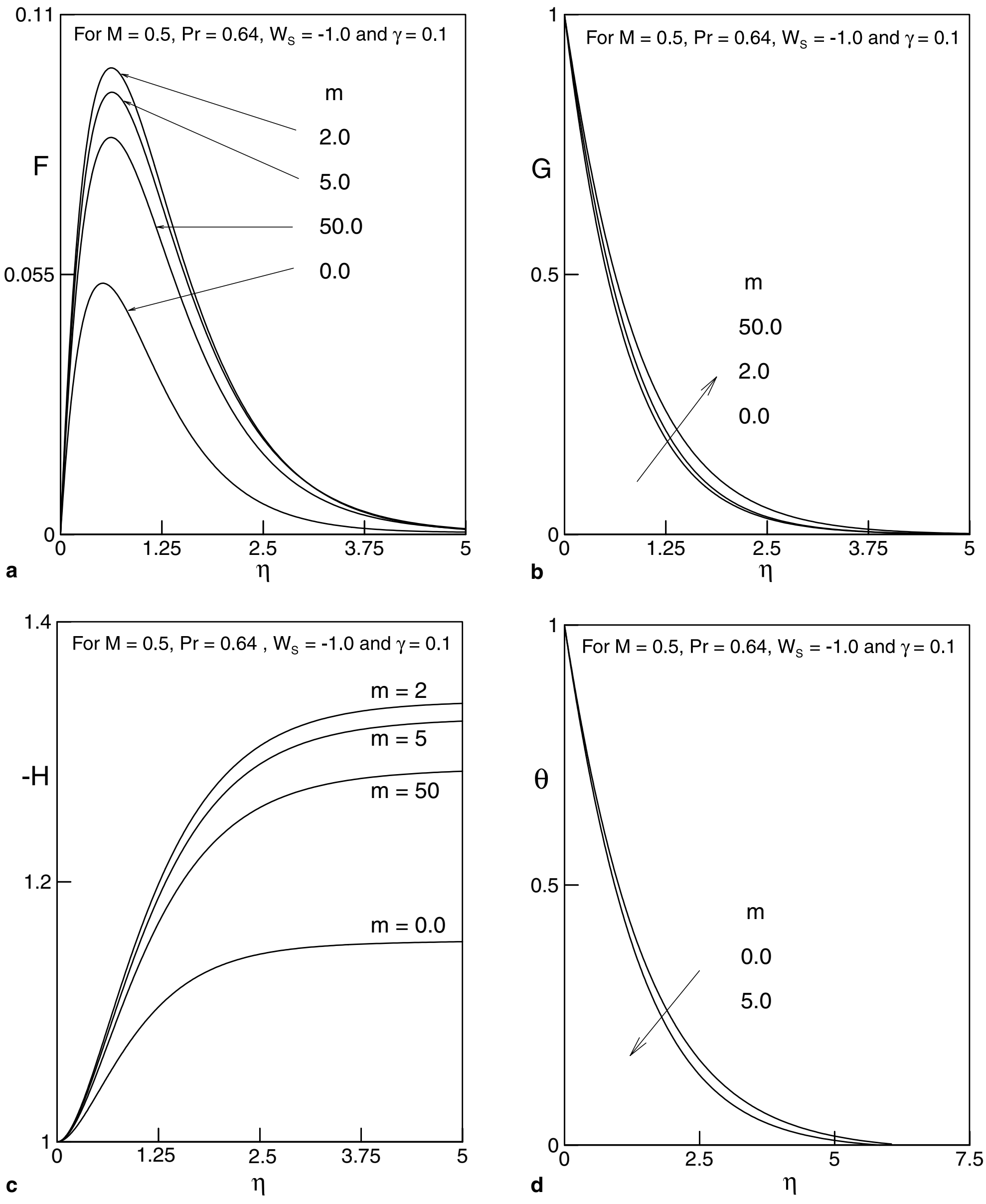

Fig. 6. (a) Effect of m on the radial velocity profiles, (b) effect of m on the tangential velocity profiles, (c) effect of m on the axial velocity profiles and (d) effect of m on the temperature velocity profiles.

blown away from the disk to form an interlayer between the injection and the outer flow regions. From Fig. 4(b) it is found that temperature decay more slowly away from the surface. As in the case of temperature difference parameter, from Fig. 4(b), we again observe that higher injection velocities have the tendency to destabilize the laminar flow. In Fig. 4(a), it is observed that for high values of injection parameter ($W_s = 4$), the radial velocity near the disk (for small values of η) is lower than that for smaller values of W_s. This is due to the fact that, with increasing values of W_s, the injected flow can sustain axial motion to greater distances from the wall. Then, near the wall, the radial flow which is fed by the axial flow is expected to decrease as the injected parameter increases.

Imposition of a magnetic field to an electrically conducting fluid creates a drag like force called the Lorentz force. This force has the tendency to slow down the flow around the disk at the expense of increasing its temperature. This is depicted by the decreases in the radial, tangential and axial velocity profiles and increases in the temperature profiles as M increases as shown in

Table 1
Numerical values of the radial and tangential skin-friction coefficients and the rate of heat transfer coefficient obtained for $Pr = 0.71$ and $M = m = \gamma = 0$

W_s	Present			Kelson and Desseaux [22]		
	$F'(0)$	$-G'(0)$	$-\theta'(0)$	$F'(0)$	$-G'(0)$	$-\theta'(0)$
4	0.2430438	0.289211e-1	0.10988e-4	0.243044	0.289211e-1	0.107326e-4
3	0.3091472	0.602891e-1	0.582267e-3	0.309147	0.602893e-1	0.576744e-3
2	0.3989332	0.1359517	0.110523e-1	0.398934	0.135952	0.110135e-1
1	0.4894776	0.3021728	0.856031e-1	0.489481	0.302173	0.848848e-1
0	0.5101430	0.6159604	0.329527	0.510233	0.615922	0.325856
−1	0.3894148	1.1756345	0.797678	0.389569	1.175222	0.793048
−2	0.2432800	2.0413676	1.450654	0.242421	2.038527	1.437782
−3	0.1668408	3.0147714	2.149055	0.165582	3.012142	2.135585
−4	0.1276609	4.0099877	2.864478	0.124742	4.005180	2.842381

Table 2
Numerical values of the radial and tangential skin-friction coefficients and the rate of heat transfer coefficient obtained for $m = M = 0.1, W_s = -1.0$ and $Pr = 0.64$

γ	$F'(0)$	$-G'(0)$	$-\theta'(0)$
−1.0	0.482014	3.336285	1.009969
−0.8	0.485064	2.776696	0.952151
−0.5	0.468276	2.086653	0.867656
−0.2	0.421738	1.538455	0.779307
0.0	0.372331	1.233757	0.720557
0.2	0.306259	0.966984	0.655588
0.5	0.168678	0.622670	0.559004
0.8	0.109027	0.518923	0.516888
1.0	−0.000367	0.370817	0.442873

Fig. 5(a)–(d). In addition, the increases in the temperature profiles as M increases are accompanied by increases in the thermal boundary layer.

If the parameters γ, W_s and M are held constants, m illustrates the effect of Hall term on the flow. The parameter m has a marked effect on the velocity profiles as seen in Fig. 6(a) and (c). It is observed that, due to an increase in the magnitude of m within 0–2.0 (not precisely determined), both radial and axial velocity profiles increase. But if the magnitude of m is increased beyond the limit of 2.0 (possibly), the velocity profiles show a decreasing effect. This is due to the fact that for large values of m, the term $1/(1 + m^2)$ is very small and hence the resistive effect of the magnetic field is diminished. This phenomenon for small and large values of m has been effectively explained by Hassan and Attia [13]. From Fig. 6(b) we observe that the Hall parameter m has slightly increasing effect on the tangential velocity profiles.

The Hall current parameter m and magnetic interaction parameter M do not enter directly into the energy Eq. (16) but its influence come through the momentum Eqs. (14) and (15). Fig. 5(d) and Fig. 6(d) show the small variation of temperature profiles for different values of M and m respectively. From Fig. 5(d), it is observed that the value of non-dimensional temperature profile increases a little with the increasing values of M and this also leads to a small rate of increase in the thermal boundary layer thickness. The temperature profile decreases with the increasing values of Hall parameter m is shown in Fig. 6(d).

Finally, the values of radial and tangential skin frictions and the rate of heat transfer have been presented in Tables 1 and 2. From Table 1, it can be seen that the values of the radial and tangential skin friction and the rate of heat transfer coefficients decrease for increasing values of injection velocity ($W_s = 0$ to 4). It also can be seen from this table that increasing the suction velocity ($W_s = 0$ to -4) leads to decrease in the radial skin friction coefficient while increase in the azimuthal (tangential) skin friction and the rate of heat transfer coefficients. It can be seen from Table 2 that the radial, the tangential and the rate of heat transfer coefficients decrease with the increasing values of temperature difference parameter γ.

7. Conclusions

In this paper, the effects of variable properties along with the effects of suction/injection and Hall current on a steady MHD convective flow induced by an infinite rotating porous disk were studied. The Nachtsheim and Swigert [20] iteration technique based on sixth-order Range–Kutta and Shooting method has been employed to complete the integration of the resulting solutions.

The following conclusions can be drawn as a result of the computations:

1. Variable properties (γ) has marked effects on the radial and axial velocity profiles. Close to the surface of the disk these velocities slow down as γ increases but shortly after they increase with the increase of γ.

2. Due to the existence of the centrifugal force, the radial velocity reaches a maximum value close to the surface of the disk.
3. Close to the boundary positive values of γ is found to give rise to the familiar inflection point profile leading to the destabilization of the laminar flow. Strong injection also leads to the similar destabilization effect.
4. The effect of Lorentz force or the usual resistive effect of the magnetic field on the velocity profiles is apparent.
5. Hall parameter m has an interesting effect on the radial and axial velocity profiles. For large values of $m(>2.0)$, the resistive effects of the magnetic field is diminished and hence the radial and axial velocity profiles decreases with the increase of m.
6. Increasing the values of $\gamma(-1.0$ to $1.0)$ lead to the decrease in radial and tangential skin friction coefficients and the rate of heat transfer coefficient for fixed values of W_s, M, m and Pr.

References

[1] J. Herrero, J.A.C. Humphrey, F. Giralt, Comparative analysis of coupled flow and heat transfer between co-rotating discs in rotating and fixed cylindrical enclosures, Am. Soc. Mech. Eng., Heat Transfer Div. 300 (1994) 111–121.
[2] J.M. Owen, R.H. Rogers, Flow and heat transfer in rotating disc system, Rotor–Stator Systems, vol. 1, Research Studies Press, Taunton, UK and John Wiley, NY, 1989.
[3] T. von Karman, Uber laminare und turbulente reibung, ZAMM 1 (1921) 233–255.
[4] W.G. Cochran, The flow due to a rotating disc, Proc. Cambridge Phil. Soc. 30 (1934) 365–375.
[5] E.R. Benton, On the flow due to a rotating disc, J. Fluid Mech. 24 (Part-4) (1965) 781–800.
[6] M.G. Roger, G.N. Lance, The rotationally symmetric flow of a viscous fluid in presence of infinite rotating disc, J. Fluid Mech. 7 (1960) 617–631.
[7] G.K. Batchelor, Note on a class of solutions of the Navier–Stokes equations representing steady non-rotationally symmetric flow, Quart. J. Mech. Appl. Math. 4 (1951) 29–41.
[8] J.T. Stuart, On the effect of uniform suction on the steady flow due to a rotating disc, Quart. J. Mech. Appl. Math. 7 (1954) 446–457.
[9] H. Ockendon, An asymptotic solution for steady flow above an infinite rotating disc with suction, Quart. J. Mech. Appl. Math. 25 (1972) 291–301.
[10] H.K. Kuiken, The effect of normal blowing on the flow near a rotating disk of infinite extent, J. Fluid Mech. 47 (4) (1971) 789–798.
[11] T.M.A. El-Mistikawy, H.A. Attia, A.A. Megahed, The rotating disk flow in the presence of weak magnetic field, in: Proc. Fourth Conf. Theoret. Appl. Mech., Cairo, Egypt, 5–7 November, 1991, pp. 69–82.
[12] T.M.A. El-Mistikawy, H.A. Attia, The rotating disk flow in the presence of strong magnetic field, in: Proc. Third int. Cong. Fluid Mech., Cairo, Egypt, 2–4 January, 3, 1990, pp. 1211–1222.
[13] A.L.A. Hassan, Hazem Ali Attia, Flow due to a rotating disk with Hall effect, Phys. Lett. A 228 (1997) 246–290.
[14] Hazem Ali Attia, Unsteady MHD flow near a rotating porous disk with uniform suction or injection, Fluid Dyn. Res. 23 (1998) 283–290.
[15] M. Zakerullah, J.A.D. Ackroyd, Laminar Natural Convection Boundary Layers on Horizontal Circular discs, J. Appl. Math. Phys. 30 (1979) 427–435.
[16] H. Herwig, The effect of variable properties on momentum and heat transfer in a tube with constant heat flux across the wall, Int. J. Heat Mass Transfer 28 (1985) 424–441.
[17] H. Herwig, G. Wickern, The effect of variable properties on laminar boundary layer flow, Warme und Stoffubertragung 20 (1986) 47–57.
[18] H. Herwig, K. Klemp, Variable property effects of fully developed laminar flow in concentric annuli, ASME J. Heat Transfer 110 (1988) 314–320.
[19] H. Herwig, An asymptotic analysis of laminar film boiling a vertical plate including variable property effects, Int. J. Heat Mass Transfer 31 (1988) 2013–2021.
[20] P.R. Nachtsheim, P. Swigert, Satisfaction of asymptotic boundary conditions in numerical solution of system of nonlinear of boundary layer type. NASA TN-D3004, 1965.
[21] S. Jayaraj, Thermophoresis in laminar flow over cold inclined plates with variable properties, Heat Mass Transfer 30 (1995) 167–173.
[22] N. Kelson, A. Desseaux, Note on porous rotating disk flow, ANZIAM J. 42(E) (2000) C837–C855.